

## A Neural Link Between Feeling and Hearing

Tony Ro<sup>1</sup>, Timothy M. Ellmore<sup>2</sup> and Michael S. Beauchamp<sup>3</sup>

<sup>1</sup>Department of Psychology and Program in Cognitive Neuroscience, The City College and Graduate Center of the City University of New York, New York, NY, USA, <sup>2</sup>Department of Neurosurgery and <sup>3</sup>Department of Neurobiology and Anatomy, University of Texas Health Science Center, Houston, TX, USA

Address correspondence to Tony Ro, Email: tro@ccny.cuny.edu

**Hearing and feeling both rely upon the transduction of physical events into frequency-based neural codes, suggesting that the auditory system may be intimately related to the somatosensory system. Here, we provide evidence that the neural substrates for audition and somatosensation are anatomically linked. Using diffusion tensor imaging with both deterministic and probabilistic tractography to measure white matter connectivity, we show that there are extensive ipsilateral connections between the primary auditory cortex and the primary and secondary somatosensory regions in the human cerebral cortex. We further show that these cross-modal connections are exaggerated between the auditory and secondary somatosensory cortex in the lesioned hemisphere of a patient (SR) with acquired auditory-tactile synesthesia, in whom sounds alone produce bodily sensations. These results provide an anatomical basis for multisensory interactions between audition and somatosensation and suggest that cross-talk between these regions may explain why some sounds, such as nails screeching down a chalkboard or an audible mosquito, can induce feelings of touch, especially on the contralesional body surface of patient SR.**

**Keywords:** brain, multisensory, sound, touch, synesthesia

### Introduction

Many sounds can induce sensations that are felt on the body, such as high-pitched screeching noises or low-frequency thumping sounds. Consistent with this phenomenology, several recent behavioral studies have demonstrated systematic perceptual interactions between the auditory and somatosensory modalities. For example, auditory sounds at one frequency affect the perception of somatosensory vibrations at the same or similar frequencies (Ro et al. 2009; Yau et al. 2009; Wilson et al. 2010), somatosensory vibrations influence the perceived intensity of auditory stimuli (Yau et al. 2010), somatosensory stimuli can influence the perception of language (Gick and Derrick 2009; Ito et al. 2009) and vice versa (Ito and Ostry 2012), and higher auditory frequencies and intensities can alter texture perception (Jousmaki and Hari 1998; Guest et al. 2002). Such results suggest the existence of highly tuned multisensory integration mechanisms for gathering consistent information about the environment, such as when hearing and feeling one's hand rubbing over textured surfaces. These interactions between audition and touch may be a consequence of several striking similarities between the auditory and somatosensory systems.

Physiologically, the similarity between auditory and somatosensory processing begins in the structure and function of the receptor organs. Both audition and touch depend upon the mechanical displacement of receptors (the stereocilia of hair cells in the cochlea for audition, the cell membrane of

mechanoreceptors for vibration in the skin) to transduce physical events into neural signals. Both modalities are also frequency-dependent, with different populations of cochlear hair cells and skin mechanoreceptors tuned to different frequencies. There is also evidence suggesting that the hair cells in the inner ear and those found in the lateral lines along the extent of the body of fish share a common ontogenetic origin (Ladher et al. 2010).

Neuroanatomically, the organization of the cerebral cortex is well suited for integrating sound and touch information because the primary auditory cortex (A1) on the superior temporal plane is located adjacent to secondary somatosensory areas in the parietal operculum. Because minimizing the number of long-distance cortico-cortical connections is essential for efficient brain function (Van Essen 1997), cortical connections between the auditory and adjacent somatosensory cortex may play a key role in the link between auditory and touch perception.

In non-human primates, anatomical studies have shown that there are direct ipsilateral cortico-cortical projections from the secondary somatosensory cortex to belt areas of the auditory cortex (Schroeder et al. 2001; Cappe and Barone 2005; Smiley et al. 2007). There is also evidence of direct ipsilateral cortico-cortical connections between the primary auditory cortex and the primary somatosensory cortex in gerbils (Budinger et al. 2006). The functional significance of these ipsilateral cortico-cortical projections has been suggested by studies in macaque monkeys showing multisensory processing of auditory and somatosensory information in cells within belt areas of the auditory cortex (Fu et al. 2003). Furthermore, studies in rats have demonstrated that lesions to the somatosensory cortex can systematically affect processing of auditory information in the auditory cortex (Escabi et al. 2007; Higgins et al. 2008).

Despite this growing literature demonstrating anatomical connectivity and physiological and behavioral interactions between the somatosensory and auditory cortices in non-human mammals, only a few studies have examined functional interactions between these cortical regions in humans. Notably, it has been shown that regions within the human auditory cortex may be responsive to touch (Fuxe et al. 2002; Kayser et al. 2005; Schurmann et al. 2006). Conversely, using functional magnetic resonance imaging (fMRI), we previously showed that regions of the secondary somatosensory cortex respond to sounds in neurologically normal humans, supporting a link between audition and touch (Beauchamp and Ro 2008). These studies suggest that anatomical connections between the auditory and somatosensory cortex may also exist in humans, but no studies to date have examined the anatomical connectivity between the human auditory and somatosensory cortex. This may be because the ability to

examine anatomical connections in the human brain was restricted to postmortem dissections until the recent development of MRI methods for measuring white matter connections. In the present study, we examined whether the existence and density of white matter fiber connections between the human somatosensory and auditory cortex could be detected using both deterministic and probabilistic tractography of diffusion-weighted MRI (Mori and Zhang 2006).

Normal humans experience sensations on their bodies only in response to some sounds, such as fingernails on a blackboard (Halpern et al. 1986). However, we have described a patient (SR) who experienced very strong sensations on her body to a variety of sounds, including pure tones, which never evoked somatosensations in normal subjects. Using MRI, we showed that this patient had a right ventrolateral thalamic lesion that deprived her somatosensory cortex of normal somatosensory input. MRI evidence suggested that over time, her somatosensory cortex became responsive to auditory stimuli because it was no longer receiving somatosensory input (Ro et al. 2007; Beauchamp and Ro 2008). A possible mechanism for this increased responsiveness would be the strengthening of normally occurring auditory–somatosensory connections, which might have become stronger in the patient because of the lack of normal thalamic inputs, resulting in her strong synesthesia. To test this idea, in the current study, we compared the density of connections between the auditory cortex and different subdivisions of the primary and secondary somatosensory cortex in neurologically normal participants and in SR. We predicted that we would find connections between the auditory and somatosensory cortex in normal subjects and that some of these connections would be stronger in SR, forming the neural underpinning of the disordered perceptual processing of sounds in this patient.

## Materials and Methods

### Subjects

Informed consent was obtained from 17 (8 females; 27.2 mean age) neurologically normal subjects and 1 female patient (41 years of age at the time of scanning) with an acquired auditory-tactile synesthesia. The patient experienced somatosensory sensations to different sounds approximately 1.5 years after a small lesion restricted to the right ventrolateral nucleus of the thalamus (for further details on this patient, see Ro et al. 2007). Apart from patient SR, none of the subjects participated in our previous fMRI study demonstrating secondary somatosensory cortex activations to sounds (Beauchamp and Ro 2008). One of the control subjects was matched in gender and was similar in age to the patient (41 vs. 40 years of age), whereas another control subject was matched in education (both had doctoral degrees), profession (both were professors), and gender with the patient. All studies were approved by the Institutional Review Boards of the City University of New York, Rice University, and the University of Texas Health Science Center at Houston.

### Methods

All subjects were scanned using a 3 T whole-body MRI scanner (Philips Medical Systems, Bothell, WA, USA) with an 8-channel parallel receiver array. High resolution T1-weighted anatomical scans were acquired with a magnetization-prepared 180° radiofrequency pulses and rapid gradient-echo (MP-RAGE) sequence optimized for gray-white matter contrast with 1-mm-thick sagittal slices [in-plane resolution = 0.938 × 0.938 mm; matrix size = 256 × 256; field of view (FOV) = 240 mm; repetition time/echo time (TR/TE) = 8.4/3.9 ms; flip angle

= 8°]. Diffusion tensor images were acquired using a 32-direction diffusion encoding scheme (high angular resolution) with the gradient overplus option. One B0 (non-diffusion weighted) image volume was acquired before the acquisition of one repetition of diffusion-weighted scans. Seventy axial slices were acquired with 2-mm slice thickness and a maximum *b*-value of 800 s/mm (in-plane resolution = 1.75 × 1.75 mm; matrix size = 128 × 128; FOV = 224 mm; TR/TE = 8500/67 ms; flip angle = 90°).

### Data Analysis

To identify anatomical regions of interest (ROIs), T1-weighted MRIs were analyzed as follows. A brain extraction algorithm was used to remove the skull and scalp from the anatomical MRI, and a 12-parameter affine transformation of each subject's anatomical scan to the T1-weighted MNI single-subject template was computed (Collins et al. 1994) and stored. ROIs in the primary auditory cortex (A1), primary somatosensory cortex (S1), and parietal opercular regions (OP1–OP4) were then created for each subject in the MNI space using the Anatomy Toolbox multiple probabilistic maps atlas (Eickhoff et al. 2005; Eickhoff et al. 2007). For S1, we separately analyzed Brodmann's areas 1, 2, 3a, and 3b, and for the secondary somatosensory cortex, we primarily focused on region OP1 because this parietal opercular region most likely corresponds to the non-human primate secondary somatosensory cortex (i.e. S2) (Eickhoff, Amunts, et al. 2006; Eickhoff, Schleicher, et al. 2006) and is the region that previous results have suggested to be critical for auditory–somatosensory interactions (Beauchamp and Ro 2008). For the primary auditory cortex, we used the parcellation scheme of Morosan et al. (2001), in which Heschl's gyrus is demarcated into three regions, TE 1.0, TE 1.1, and TE 1.2, all of which are considered together as “primary auditory cortex.”

The ROIs were dilated by 10 mm to ensure inclusion of white matter and any overlap between two masks was removed. Although there are no anatomical landmarks or multiple probabilistic maps in humans that delineate the caudal belt and parabelt regions of the auditory cortex, which have previously been shown to be anatomically and functionally linked with somatosensory areas (Schroeder et al. 2001; Fu et al. 2003), the dilation procedure likely extended the primary auditory cortex ROI into these belt areas. The ROIs in the MNI space were then reverse transformed back into the native space using the inverse of the 12-parameter affine transformation to avoid the introduction of any distortions to the DTI data (i.e. all analyses on the DTI scans were done in the native space rather than the MNI space). All masks were binary masks and were visually inspected in the native space to ensure appropriate alignment.

In an initial pre-processing step, the diffusion-weighted images were aligned to the structural T1-weighted scan for each subject using the *3dAllineate* command in the AFNI package (Cox 1996). Head motion was minimal in the patient ( $x = -0.15$  mm;  $y = -0.36$  mm;  $z = -0.44$  mm) and the controls ( $x = -1.31$  mm;  $y = 2.25$  mm;  $z = 1.32$  mm). Prior to deterministic tractography, image distortions caused by eddy currents in the MR gradients were accounted for by rotation of the *b*-matrix (Leemans and Jones 2009).

Deterministic fiber tracking was conducted with DTIQuery v1.1 using the streamline tracking algorithm (STT) (Basser et al. 2000; Akers et al. 2004; Sherbondy et al. 2005) and the following fiber tracking parameters: Path step size = 1.0 mm, seed point spacing = 2.0 mm, fractional anisotropy (FA) termination threshold = 0.15, angle termination threshold = 45°, min pathway length = 5.0 mm, max pathway length = 300.0 mm, and Euler's method for STT numerical integration. Custom written Matlab and C++ routines were used to extract the fiber tracts and the FAs between each of the ROIs in each subject.

We first measured whether any fibers between A1 and OP1/S2 could be detected using the deterministic tractography algorithms. The number of fibers for deterministic tractography between A1 and OP1/S2 was then computed for each hemisphere and used as a dependent variable in the main analyses comparing connectivity differences between the patient and the neurologically normal controls. Next, a connectivity asymmetry index was computed for each subject by subtracting the number of left hemisphere fiber tracts from the

number of right hemisphere fiber tracts and dividing this difference by the sum of the left and right fiber tracts. This produced values ranging from  $-1$ , indicating only left hemisphere connections between the auditory and somatosensory cortex, to  $0$ , indicating an equal number of left and right hemisphere connections, and to  $+1$ , indicating only right hemisphere connections between the two regions. A similar analysis was conducted on the FA values.

Probabilistic tractography (Smith et al. 2004; Behrens et al. 2007), using FSL version 4.1.9, was performed between pairs of regions specified by the same masks used for deterministic tractography and created at the resolution of the T1-weighted anatomical volume. Tracking between A1 and OP1/S2 was carried out for each hemisphere using a two-stage process that involved three masks. First, OP1/S2 was designated as the seed space mask and A1 was designated as a waypoint inclusion mask. All voxels in brain regions outside the A1 and OP1/S2 masks were specified in an exclusion mask. Tracking was performed with these three masks using standard parameters (5000 samples, 2000 steps, 0.5 mm step length, curvature threshold 0.2, pathways discarded that travel back to a point already visited) in order to select pathways that pass between A1 and OP1/S2 and to discard any pathway that entered any region of the exclusion mask. In the second stage, A1 was designated as the seed space mask and OP1/S2 the waypoint inclusion mask. Tracking was performed again with the same exclusion mask criterion. The number of voxels in the connectivity distributions from these two tracking steps was used as the dependent variable and to create a probabilistic asymmetry index similar to the one used for the deterministic data.

## Results

Because our previous fMRI study showed greater activation in OP1/S2 in response to sounds (Beauchamp and Ro 2008), our initial analysis focused on connections between the primary auditory cortex (A1) and the secondary somatosensory cortex (OP1/S2). To measure connectivity, we used two independent methods: Deterministic tractography, which computes streamlines (putative nerve fiber pathways) based on the principal diffusion directions in white matter between areas that are above an FA threshold, and probabilistic tractography, which generates estimates of the likelihood of connections between areas.

### Deterministic Tractography

In control subjects, fiber pathways were observed between A1 and OP1/S2 in both hemispheres (Fig. 1 and Table 1). In patient SR, we also observed fiber tracts between A1 and OP1/S2, but they were strongly asymmetrical: SR had significantly more connections in the lesioned right hemisphere than in the left hemisphere ( $\chi^2 = 12.25$ ,  $P < 0.001$ ). Controls showed no asymmetry in the A1 and OP1/S2 connections between the two hemispheres [ $t(16) < 1$ , NS]. To further quantify this difference, we computed an asymmetry index and compared the value of this index between the controls and the patient using a two-sample  $t$ -test with the error term from the controls and the degrees of freedom adjusted to account for the between-subject comparison. SR was significantly right-lateralized, whereas the controls were not (0.88 in SR vs.  $-0.03$  in controls) [ $t(16) = 2.30$ ,  $P = 0.035$ ]. This significant asymmetry in SR was driven by both a larger number of fibers in the right hemisphere and a smaller number of fibers in the left hemisphere.

A similar analysis was conducted on the FA values computed from the deterministic fiber tracks between A1 and OP1/S2. As with the fiber counts, patient SR had a higher FA for right hemisphere fibers between A1 and OP1/S2 when

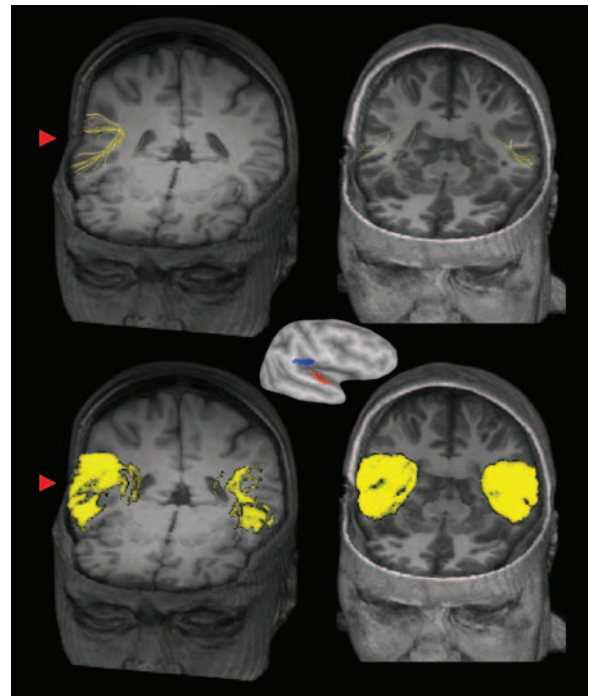


**Figure 1.** Center: Lateral view of an inflated right hemisphere (dark gray shows sulcal depths, light gray shows gyral crowns) showing ROIs used for tractography (primary auditory cortex, A1, in red; secondary somatosensory cortex, OP1/S2, in blue). Top row: Deterministic tractography results in SR (left, volume rendering with axial cutout at  $z = 1$ , coronal cutout at  $y = 45$ ) and a gender- and age-matched representative control subject (right, axial cutout at  $z = -11$ , coronal cutout at  $y = 31$ ). Individual yellow streamlines show the location of fiber tracts between A1 and OP1/S2. The red arrowhead highlights the more extensive connections between A1 and OP1/S2 in the patient's lesioned right hemisphere when compared with her contralesional hemisphere. Bottom row: Probabilistic tractography results in SR (left) and control subject (right). Yellow regions show volume rendering of individual voxels with an above threshold probability of connections between seed regions A1 and OP1/S2. The red arrowhead highlights the large number of connected voxels in SR's right hemisphere. Note the similar asymmetry between the lesioned and non-lesioned hemisphere in SR but not the control subject for both deterministic and probabilistic analyses.

compared with the left hemisphere (0.45 vs. 0.29), but this difference in FA values was only marginally significant ( $\chi^2 = 3.69$ ,  $P = 0.055$ ). In contrast, the control subjects had similar left and right hemisphere FA values for fibers between A1 and OP1/S2 [ $t(16) < 1$ , NS]. Importantly, as with the fiber counts, an asymmetry index comparison between the patient and the controls showed a significant difference, with a rightward asymmetry for SR but not for the controls [ $t(16) = 2.43$ ,  $P = 0.027$ ].

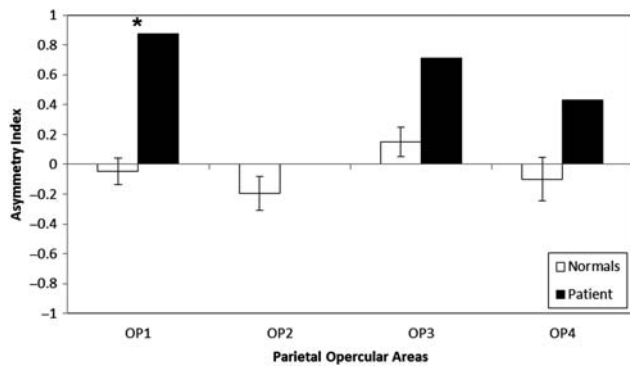
### Probabilistic Tractography

A probabilistic tractography analysis was also conducted to verify the key findings of connections between the auditory and secondary somatosensory cortex and significant hemispheric asymmetry in the patient but not the controls. The probability distributions showed a high probability of connections between the auditory and somatosensory cortex in controls (Fig. 1), with no difference in the number of voxels in the probability distributions between the left and right hemispheres [ $t(16) < 1$ , NS]. In patient SR, there was a very different pattern in the lesioned right hemisphere compared with the left hemisphere, with a larger number of voxels in the

**Table 1**ROI volumes (in mm<sup>3</sup>) and number of deterministic tractography fiber counts between the primary auditory cortex and different somatosensory cortex regions in patient SR and the control subjects

| Region | Patient SR  |       |        |       | Normals     |              |            |             |
|--------|-------------|-------|--------|-------|-------------|--------------|------------|-------------|
|        | ROI volumes |       | Fibers |       | ROI volumes |              | Fibers     |             |
|        | Left        | Right | Left   | Right | Left        | Right        | Left       | Right       |
| BA1    | 42082       | 36907 | 11     | 9     | 48902 (770) | 44827 (763)  | 3.2 (1.01) | 8.8 (1.32)  |
| BA2    | 51265       | 52960 | 17     | 10    | 43918 (986) | 45838 (1031) | 6.8 (1.18) | 12.0 (2.24) |
| BA3a   | 40225       | 38094 | 5      | 2     | 33121 (886) | 32191 (749)  | 9.8 (1.08) | 8.2 (0.99)  |
| BA3b   | 45794       | 48887 | 7      | 8     | 43535 (786) | 49692 (1135) | 5.7 (0.67) | 7.2 (1.15)  |
| OP1    | 17053       | 15076 | 1      | 15    | 15358 (289) | 13030 (298)  | 8.1 (0.77) | 8.7 (1.35)  |
| OP2    | 5074        | 5404  | 1      | 0     | 4048 (91)   | 4577 (130)   | 6.9 (0.69) | 4.5 (0.74)  |
| OP3    | 9945        | 9271  | 1      | 6     | 8980 (202)  | 8312 (173)   | 5.6 (0.87) | 7.2 (0.77)  |
| OP4    | 17596       | 14556 | 2      | 5     | 15727 (332) | 13219 (266)  | 4.4 (0.78) | 2.5 (0.50)  |

Values in parentheses for the control subjects represent 1 standard error of the mean.

**Figure 2.** Connection asymmetry from deterministic tractography between A1 and each of the four parietal opercular areas for control subjects (open bars) and patient SR (filled bars). Error bars for the control subjects represent 1 standard error of the mean, and asterisk denotes a significant difference between patient SR and the controls at  $P < 0.05$ .

probability distributions in the right hemisphere when compared with her left hemisphere ( $\chi^2 = 2813.24$ ,  $P < 0.001$ ). The difference between the patient and the neurologically normal control subjects was quantified by computing an asymmetry index. Consistent with the results from deterministic tractography, SR was significantly right-lateralized, whereas the controls were not (0.61 in SR vs. 0.02 in controls) [ $t(16) = 2.65$ ,  $P = 0.017$ ].

### Additional Regions and Analyses

We also used deterministic tractography to examine connections between the primary auditory cortex and other somatosensory regions. Although connections were detected in both the patient and the controls between A1 and the other parietal opercular regions (i.e. OP2, OP3, OP4; Table 1), unlike OP1/S2, there were no statistically significant asymmetries or differences between the patient and the controls for these other parietal opercular subdivisions (all  $P$ 's > 0.10; Fig. 2 and Table 1). For connections between the primary auditory cortex and the primary somatosensory cortex (S1), we first subdivided each subject's S1 into Brodmann's areas 1, 2, 3a, and 3b and then computed the number of fiber tracks between A1 and each of the different S1 regions. As with the parietal opercular regions, fiber tracts were detected between A1 and S1 in both the patient and the controls (Fig. 3 and Table 1). There were no significant fiber count hemispheric asymmetries in the A1 and S1 connections for both the

patient and the controls (all  $P$ 's > 0.10). However, on visual inspection (Fig. 3), the connections between A1 and S1 in the patient's lesioned hemisphere appeared sparse with a different spatial configuration than in the contralesional hemisphere and compared with controls (cf. Ro et al. 2007).

A correlation analysis was conducted to determine whether the volume of the different ROIs might affect the number of deterministic tractography fibers detected. For this analysis, we included the number of fibers between A1 and each of the eight somatosensory regions (OP1, OP2, OP3, OP4, BA1, BA2, BA3a, and BA3b) in each hemisphere for the normal control subjects and patient SR. Although there was no relationship between the ROI volume and the mean number of fiber counts in the left and right hemispheres of the control subjects ( $r = -0.19$ ,  $P > 0.10$  and  $r = 0.60$ ,  $P = 0.11$ , respectively), there was a significant positive correlation between the ROI volume and the number of fibers in the left hemisphere of patient SR ( $r = 0.86$ ,  $P = 0.006$ ), but not in the lesioned right hemisphere ( $r = 0.27$ ,  $P > 0.10$ ). Thus, our results showing a greater number of fibers between A1 and OP1/S2 in the right but not left hemisphere of patient SR cannot simply be attributed to differences in ROI volume size (Table 1).

These additional analyses on S1, as well as those conducted on the additional parietal opercular subdivisions, serve as negative controls for our main finding of an asymmetry between A1 and OP1/S2 in the patient, but not the control subjects.

## Discussion

### Connections Between the Auditory and Somatosensory Cortex: Normal Brains

Using both deterministic and probabilistic tractography, we show the existence of fiber connections between the primary auditory cortex in the temporal lobe and several different somatosensory regions in the parietal lobe, including the primary somatosensory cortex as well as the secondary somatosensory cortex in the parietal operculum. The consistency of these results, specifically of those between A1 and OP1/S2, across several different dependent variables and tractography analyses indicates that these fiber connections are robust and not simply due to some artifact or limitation in the analysis technique (e.g. the selection of a principal eigenvector in deterministic tractography or multiple pathways in probabilistic tractography, see Ellmore et al. 2011 for further direct

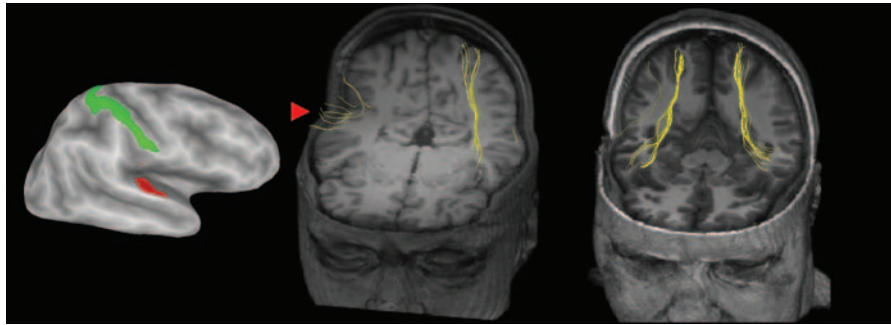


**Figure 3.** Left: Lateral view of an inflated right hemisphere (dark gray shows sulcal depths, light gray shows gyral crowns) showing ROIs used for tractography (primary auditory cortex, A1, in red; postcentral gyrus, the location of the primary somatosensory cortex, S1, in green). Deterministic tractography results in SR (middle, volume rendering with axial cutout at  $z = 1$ , coronal cutout at  $y = 67$ ) and a gender- and age-matched control subject (right, axial cutout at  $z = -14$ , coronal cutout at  $y = 39$ ). Individual yellow streamlines show the inferred location of fiber tracts between A1 and S1. The red arrowhead highlights the sparse and disorganized connections between A1 and S1 in the patient's lesioned right hemisphere.

comparisons). Thus, these consistently measured connections between the auditory and somatosensory cortex may be the human analog of those measured using invasive anatomical and physiological techniques in the belt areas of monkey auditory cortex (Schroeder et al. 2001; Fu et al. 2003; Cappe and Barone 2005; Smiley et al. 2007) and suggest a direct neural link between the sensations of audition and touch.

In a series of psychophysical experiments in neurologically normal subjects, we have shown that sounds can affect touch perception in spatially dependent and frequency-specific ways (Ro et al. 2009). When a sound was presented on the same side as a near-threshold electrical cutaneous stimulus, detection rates increased when compared with when the sound was presented on the opposite side from the touch. We also showed that when a non-informative sound was presented along with a near-threshold vibrotactile stimulus delivered to the hand, the sound increased touch perception if it was at the same frequency as the vibrotactile stimulus (also see Wilson et al. 2010). One potential neural basis for these effects of sounds on touch perception may be interconnections between the auditory and somatosensory cortex. These connections may also be strengthened as a result of their use, similar to diffusion-weighted imaging changes following other sorts of adult brain plasticity (Carreiras et al. 2009).

In normal subjects, fMRI responses have been observed in the secondary somatosensory cortex to sounds (Beauchamp and Ro 2008). However, fMRI does not have the temporal resolution to determine the sequence of activation of different cortical areas. One obvious suggestion of our study is that auditory stimuli first evoke activity in the auditory cortex, and this activity then spreads via these cortico-cortical connections to the somatosensory cortex. Studies using techniques with better temporal resolution, such as transcranial magnetic stimulation (Bolognini and Ro 2010), electroencephalography, or fast signal optical imaging (Gratton and Fabiani 1998; Gratton and Fabiani 2010), could be informative in assessing the temporal dynamics of these neural activations.

#### **Connections Between the Auditory and Somatosensory Cortex: Patient SR**

We also observed auditory–somatosensory connections in patient SR, who after a right ventrolateral nucleus lesion feels sensations on her body in response to sounds, especially on her left hand and arm. A disproportionately larger number of

fibers were measured in the patient's ipsilesional hemisphere between A1 and OP1/S2 when compared with the normal control subjects. These results, in conjunction with our previous fMRI findings of activation of the secondary somatosensory cortex in response to sounds (Beauchamp and Ro 2008), suggest that anatomical as well as functional changes may be underlying these synesthetic sensory changes in the patient.

The finding that the A1 to OP1/S2 connections are more abundant in the lesioned hemisphere of patient SR when compared with normals provides an anatomical basis for the auditory-tactile synesthesia observed in this patient. After the patient's right ventrolateral thalamic nucleus lesion and her associated unilateral somatosensory deficits, it is likely that her secondary somatosensory cortex, deprived of its normal input, began to reorganize to receive greater input from the nearby auditory cortex. Interestingly, patient SR had an equal number of, but more sporadic, fiber tracts between A1 and S1, likely a consequence of deprived cortical input from the thalamus (Ro et al. 2007). Since there was a large numerical asymmetry difference between the normal brains and the lesioned patient's brain only in OP1/S2, these results suggest that axonal sprouting, rather than the unmasking of existing connections, may be taking place between proximal regions of the brain after deprived input or after extensive experience. Because the thalamic lesion in the patient was restricted to the ventrolateral nucleus, and also because of the apparent asymmetry in A1 and S1 connections, we believe that most of the plasticity in patient SR is due to more local changes in cortical connections between the auditory and somatosensory cortex rather than thalamocortical changes from the ventrolateral nucleus of the thalamus to premotor cortex or the ventral posterolateral nucleus of the thalamus to primary somatosensory or secondary somatosensory cortices (Friedman and Murray 1986).

Although the larger number of auditory cortex connections between A1 and OP1/S2 in the lesioned hemisphere of patient SR could be an artifact of the DTI fiber tracking algorithms used in this study, which are more effective at detecting shorter fibers with fewer bends, we feel that these results are not an artifact of the methods for several reasons. First, these asymmetries were restricted to OP1/S2 and consistently measured using several different fiber tracking algorithms. Second, the increased number of these fibers is consistent with the finding that the caudomedial belt areas of the

auditory cortex primarily process both auditory and somatosensory information; these multisensory processes in the caudal portion of the primary auditory cortex and/or belt areas make these regions likely candidates for cross-modal plasticity after deprived input, as in patient SR. Third, because A1 is adjacent to OP1/S2, this proximity would allow for faster processing times, more compact and less complex neuronal architecture (e.g. connections with fewer fiber crossings), and may promote other types of structural changes that are functionally dependent, such as axonal sprouting. Regions that are anatomically closer to one another in the brain are likely to have similar functions and more extensive connections and interactions between them. Finally, the asymmetry between the ipsilesional and contralesional hemispheres within one brain is not easily explained by an artifact of any algorithm or method.

Based on these results and considerations, our working hypothesis is that following damage to SR's right thalamus, her right somatosensory cortex no longer received direct somatosensory input, as reflected in her insensitivity to touch and earlier DTI scans taken on this patient (Ro et al. 2007). Because the sensorimotor cortex was deprived of thalamic input, connections between A1 and S1 became more sporadic on the lesioned side, but connections between A1 and OP1/S2 became more responsive to already existing auditory–somatosensory connections. This suggests that following brain damage, directly connected regions to the lesion may degenerate, but that indirectly connected regions may be involved with reorganizing to compensate for the damage.

Two limitations of our study are that DTI is an indirect measure of neuronal connections with many assumptions, unlike studies using retrograde tracers, and the use of a single case to examine structural differences underlying a rare condition limits the generalizability of these findings. Future studies that use more direct anatomical measures, such as those using stains and tracers to measure cell counts and axonal connectivity, as well as studies using a larger number of patients, will be important to validate some of these findings and to confirm these hypotheses. Interestingly, a new case of auditory–tactile synesthesia, among other types of synesthesia, after a thalamic stroke has recently been reported (Fornazzari et al. 2011), providing some evidence that the occurrence of acquired synesthesia after a thalamic lesion is not an idiosyncrasy of a single patient, but perhaps a more general consequence of certain types of thalamic lesions. Whether this new patient has altered auditory–somatosensory cortex connections remains to be determined, as does the critical thalamic lesion location for producing acquired synesthesia.

### **Implications for Multisensory Interactions**

These connections between the primary auditory cortex and several somatosensory cortex regions suggest that multisensory processing occurs in brain areas traditionally conceived of as being unisensory. In conjunction with other anatomical studies that have also shown projections from the auditory cortex into the primary visual cortex (Falchier et al. 2002; Rockland and Ojima 2003), these results suggest that even areas as early as the primary sensory cortices may be processing information from multiple sensory modalities and that

much of the neocortex may be multisensory (Ghazanfar and Schroeder 2006).

The proximity and connectivity between A1 and the secondary somatosensory cortex, along with the similar frequency-based processing mechanisms between audition and touch and their common genetic origin (Ladher et al. 2010), suggest that the sense of hearing may have evolved from the sense of feeling, allowing for the extraction of information from the extrapersonal space. Indeed, a recent twin study provides evidence that touch sensitivity is heritable and correlated with hearing acuity (Frenzel et al. 2012). Further support for this sensory evolution hypothesis comes from a recent study that provides convincing evidence that the middle ear bones evolved from bones in the jaw (Meng et al. 2011) and that cells in the inner ear and those found in the lateral lines of fish share a common genetic origin. This latter result suggests that the lateral line (and cochlea) used to detect air/water vibrations originally evolved from the mechanoreceptors used for direct sensation of touch. Thus, in addition to feeling displacements of the skin, most species now possess the ability to hear sounds through similar displacements of the tympanic membrane that trigger hair cell responses in the cochlea. These genetically and evolutionary common origins for hearing and touch may also be why our senses are so well integrated with one another and why certain sounds, such as nails screeching down a chalkboard, may evoke strong bodily sensations.

### **Funding**

This research was supported by NSF grants BCS 0642801, BCS 0847607, and EFRI 1137172 to T.R., BCS 0642532 to M.S.B., and NIH grant 5R01NS065395 to M.S.B.

### **References**

- Akers D, Sherbondy A, Mackenzie R, Dougherty R, Wandell B. 2004. Exploration of the brain's white matter pathways with dynamic queries. In: Proceedings of the conference on visualization '04 (VIS '04). IEEE Computer Society, Washington, DC, USA, 377–384. doi: 10.1109/VISUAL.2004.30. <http://dx.doi.org/10.1109/VISUAL.2004.30>.
- Basser PJ, Pajevic S, Pierpaoli C, Duda J, Aldroubi A. 2000. In vivo fiber tractography using DT-MRI data. *Magn Reson Med*. 44:625–632.
- Beauchamp MS, Ro T. 2008. Neural substrates of sound–touch synesthesia after a thalamic lesion. *J Neurosci*. 28:13696–13702.
- Behrens TE, Berg HJ, Jbabdi S, Rushworth MF, Woolrich MW. 2007. Probabilistic diffusion tractography with multiple fibre orientations: what can we gain? *Neuroimage*. 34:144–155.
- Bolognini N, Ro T. 2010. Transcranial magnetic stimulation: disrupting neural activity to alter and assess brain function. *J Neurosci*. 30:9647–9650.
- Budinger E, Heil P, Hess A, Scheich H. 2006. Multisensory processing via early cortical stages: connections of the primary auditory cortical field with other sensory systems. *Neuroscience*. 143:1065–1083.
- Cappe C, Barone P. 2005. Heteromodal connections supporting multisensory integration at low levels of cortical processing in the monkey. *Eur J Neurosci*. 22:2886–2902.
- Carreiras M, Seghier ML, Baquero S, Estevez A, Lozano A, Devlin JT, Price CJ. 2009. An anatomical signature for literacy. *Nature*. 461:983–986.
- Collins DL, Neelin P, Peters TM, Evans AC. 1994. Automatic 3D inter-subject registration of MR volumetric data in standardized Talairach space. *J Comput Assist Tomogr*. 18:192–205.

- Cox RW. 1996. AFNI: software for analysis and visualization of functional magnetic resonance neuroimages. *Comput Biomed Res.* 29:162–173.
- Eickhoff S, Stephan K, Mohlberg H, Grefkes C, Fink G, Amunts K, Zilles K. 2005. A new SPM toolbox for combining probabilistic cytoarchitectonic maps and functional imaging data. *Neuroimage.* 25:1325–1335.
- Eickhoff SB, Amunts K, Mohlberg H, Zilles K. 2006. The human parietal operculum. II. Stereotaxic maps and correlation with functional imaging results. *Cereb Cortex.* 16:268–279.
- Eickhoff SB, Grefkes C, Zilles K, Fink GR. 2007. The somatotopic organization of cytoarchitectonic areas on the human parietal operculum. *Cereb Cortex.* 17:1800–1811.
- Eickhoff SB, Schleicher A, Zilles K, Amunts K. 2006. The human parietal operculum. I. Cytoarchitectonic mapping of subdivisions. *Cereb Cortex.* 16:254–267.
- Ellmore TM, Pieters TA, Tandon N. 2011. Dissociation between diffusion MR tractography density and strength in epilepsy patients with hippocampal sclerosis. *Epilepsy Res.* 93:197–203.
- Escabi MA, Higgins NC, Galaburda AM, Rosen GD, Read HL. 2007. Early cortical damage in rat somatosensory cortex alters acoustic feature representation in primary auditory cortex. *Neuroscience.* 150:970–983.
- Falchier A, Clavagnier S, Barone P, Kennedy H. 2002. Anatomical evidence of multimodal integration in primate striate cortex. *J Neurosci.* 22:5749–5759.
- Fornazzari L, Fischer CE, Ringer L, Schweizer TA. 2011. “Blue is music to my ears”: multimodal synesthesias after a thalamic stroke. *Neurocase.* doi: 10.1080/13554794.2012.667123.
- Foxe JJ, Wylie GR, Martinez A, Schroeder CE, Javitt DC, Guilfoyle D, Ritter W, Murray MM. 2002. Auditory-somatosensory multisensory processing in auditory association cortex: an fMRI study. *J Neurophysiol.* 88:540–543.
- Frenzel H, Bohlender J, Pinsker K, Wohlleben B, Tank J, Lechner SG, Schiska D, Jaijo T, Ruschendorf F, Saar K *et al.* 2012. A genetic basis for mechanosensory traits in humans. *PLoS Biology.* 10:1–15.
- Friedman DP, Murray EA. 1986. Thalamic connectivity of the second somatosensory area and neighboring somatosensory fields of the lateral sulcus of the macaque. *J Comp Neurol.* 252:348–373.
- Fu KM, Johnston TA, Shah AS, Arnold L, Smiley J, Hackett TA, Garaghty PE, Schroeder CE. 2003. Auditory cortical neurons respond to somatosensory stimulation. *J Neurosci.* 23:7510–7515.
- Ghazanfar AA, Schroeder CE. 2006. Is neocortex essentially multisensory? *Trends Cogn Sci.* 10:278–285.
- Gick B, Derrick D. 2009. Aero-tactile integration in speech perception. *Nature.* 462:502–504.
- Gratton G, Fabiani M. 1998. Dynamic brain imaging: event-related optical signal (EROS) measures of the time course and localization of cognitive-related activity. *Psychon Bull Rev.* 5:535–563.
- Gratton G, Fabiani M. 2010. Fast optical imaging of human brain function. *Front Hum Neurosci.* 4:1–9.
- Guest S, Catmur C, Lloyd D, Spence C. 2002. Audiotactile interactions in roughness perception. *Exp Brain Res.* 146:161–171.
- Halpern DL, Blake R, Hillenbrand J. 1986. Psychoacoustics of a chilling sound. *Percept Psychophys.* 39:77–80.
- Higgins NC, Escabi MA, Rosen GD, Galaburda AM, Read HL. 2008. Spectral processing deficits in belt auditory cortex following early postnatal lesions of somatosensory cortex. *Neuroscience.* 153:535–549.
- Ito T, Ostry DJ. 2012. Speech sounds alter facial skin sensation. *J Neurophysiol.* 107:442–447.
- Ito T, Tiede M, Ostry DJ. 2009. Somatosensory function in speech perception. *Proc Natl Acad Sci USA.* 106:1245–1248.
- Jousmaki V, Hari R. 1998. Parchment-skin illusion: sound-biased touch. *Curr Biol.* 8:R190.
- Kayser C, Petkov CI, Augath M, Logothetis NK. 2005. Integration of touch and sound in auditory cortex. *Neuron.* 48:373–384.
- Ladher RK, O’Neill P, Begbie J. 2010. From shared lineage to distinct functions: the development of the inner ear and epibranchial placodes. *Development.* 137:1777–1785.
- Leemans A, Jones DK. 2009. The B-matrix must be rotated when correcting for subject motion in DTI data. *Magn Reson Med.* 61:1336–1349.
- Meng J, Wang Y, Li C. 2011. Transitional mammalian middle ear from a new Cretaceous Jehol eutriconodont. *Nature.* 472:181–185.
- Mori S, Zhang J. 2006. Principles of diffusion tensor imaging and its applications to basic neuroscience research. *Neuron.* 51:527–539.
- Morosan P, Rademacher J, Schleicher A, Amunts K, Schormann T, Zilles K. 2001. Human primary auditory cortex: cytoarchitectonic subdivisions and mapping into a spatial reference system. *Neuroimage.* 13:684–701.
- Ro T, Farne A, Johnson RM, Wedeen V, Chu Z, Wang ZJ, Hunter JV, Beauchamp MS. 2007. Feeling sounds after a thalamic lesion. *Ann Neurol.* 62:433–441.
- Ro T, Hsu J, Yasar NE, Elmore LC, Beauchamp MS. 2009. Sound enhances touch perception. *Exp Brain Res.* 195:135–143.
- Rockland KS, Ojima H. 2003. Multisensory convergence in calcarine visual areas in macaque monkey. *Int J Psychophysiol.* 50:19–26.
- Schroeder CE, Lindsley RW, Specht C, Marcovici A, Smiley JF, Javitt DC. 2001. Somatosensory input to auditory association cortex in the macaque monkey. *J Neurophysiol.* 85:1322–1327.
- Schurmann M, Caetano G, Hlushchuk Y, Jousmaki V, Hari R. 2006. Touch activates human auditory cortex. *Neuroimage.* 30:1325–1331.
- Sherbondy A, Akers D, Mackenzie R, Dougherty R, Wandell B. 2005. Exploring connectivity of the brain’s white matter with dynamic queries. *IEEE Trans Vis Comput Graph.* 11:419–430.
- Smiley JF, Hackett TA, Ulbert I, Karmas G, Lakatos P, Javitt DC, Schroeder CE. 2007. Multisensory convergence in auditory cortex, I. Cortical connections of the caudal superior temporal plane in macaque monkeys. *J Comp Neurol.* 502:894–923.
- Smith SM, Jenkinson M, Woolrich MW, Beckmann CF, Behrens TE, Johansen-Berg H, Bannister PR, De Luca M, Drobnjak I, Flitney DE *et al.* 2004. Advances in functional and structural MR image analysis and implementation as FSL. *Neuroimage.* 23(Suppl. 1): S208–S219.
- Van Essen DC. 1997. A tension-based theory of morphogenesis and compact wiring in the central nervous system. *Nature.* 385:313–318.
- Wilson EC, Reed CM, Braida LD. 2010. Integration of auditory and vibrotactile stimuli: effects of frequency. *J Acoust Soc Am.* 127:3044–3059.
- Yau J, Weber AI, Bensmaia SJ. 2010. Separate mechanisms for audio-tactile pitch and loudness interactions. *Front Psychol.* 1:1–11.
- Yau JM, Olenczak JB, Dammann JF, Bensmaia SJ. 2009. Temporal frequency channels are linked across audition and touch. *Curr Biol.* 19:561–566.